

Evaluation of Different ADS Material Concepts using Various Safety Metrics

William Thomas Hollowell, Ph.D.

WTH Consulting LLC

Rudolf Reichert

Steve Kan, Ph.D.

Chung-Kyu Park, Ph.D.

George Mason University

United States

Paper Number 23-0251

ABSTRACT

Research Question/Objective: New vehicle concepts of occupied and un-occupied Automated Driving Systems [(U)ADS] are fast evolving. Their design, materials used, and energy absorbing structures can significantly differ from traditional vehicles. Appropriate analysis methods and safety metrics can help to evaluate their crashworthiness and compatibility when colliding with other vehicles or road-side hardware. This paper explores the effect different material concepts of an ADS vehicle's outer body has on self-protection and partner protection. The research is considered an example to demonstrate how various impact configurations and simulation analysis tools and metrics can be used to assess structural and occupant aspects for this new type of vehicle class.

Methods and Data Sources: Previously developed Finite Element (FE) models of generic ADS vehicles in combination with validated road-side hardware, crash barrier, and occupants were used to understand the effect different material concepts can have on self- and partner-protection. Partner-protection was analyzed using EuroNCAP's mobile progressive deformable barrier (MPDB) and its respective compatibility metric Occupant Load Criterion (OLC), where lower values represent better compatibility. Self-protection was studied using occupant injury metrics recorded during a run-off road impact scenario, where the ADS vehicles impacted a New Jersey Barrier (NJB).

Results: Differences in crash compatibility were observed depending on the material concepts used. The impact of a mid-size ADS vehicle using thermoplastic material for select components with the MPDB resulted in an OLC value of 18. The same vehicle with a composite material concept showed an OLC value of 19, while an OLC value of 22 was recorded for the baseline vehicle with a steel material concept. Differences in occupant metrics HIC, BRIC, chest deflection, and femur loads were small when comparing the three material concepts in a 35-mph oblique impact into a NJB.

Discussion and Limitations: The use of different material concepts resulted in different total vehicle mass. The vehicle using thermoplastic material for select components had a mass of 3,653 kg. The same vehicle with composite material concept had a mass of 3,718 kg, while the baseline vehicle using steel had a mass of 4,273 kg. Lower vehicle mass correlated with better partner-protection based on OLC metrics. Occupant metrics were mainly affected by the interior concept, which was identical for all three vehicles. Differences in occupant load was therefore small. The same vehicle design and underlying structure was used during this study and no optimization towards the respective material concept was performed.

Conclusions and Relevance to Session Submitted: The research is relevant to demonstrate how simulation tools can contribute to assessing this new type of ADS vehicle class. Material concepts that resulted in a smaller vehicle mass tended to show better partner protection. The interior concept, which was the same for all three ADS vehicle variations, was the main factor for producing similar occupant injury metrics for the evaluated impact scenario.

INTRODUCTION

In perpetuation of successful research collaboration for more than a decade ^{1,2,3}, the American Chemistry Council (ACC) and the George Mason University (GMU) continued to conduct research to understand opportunities for using plastics and composite materials for future automated vehicles.

Automated Driving Systems (ADS) have the potential of significantly reducing fatalities and serious injuries by reducing the number crashes on US roadways. These new technologies, however, may present unique challenges for protecting occupants in the remaining crashes that still occur. New ADS are expected to include new vehicle types that are configured to carry cargo or occupants or both. Current vehicles are designed to have their crash response in accordance with the Federal Motor Vehicle Safety Standard (FMVSS) occupant protection standards. Crash configuration of fully automated vehicles can be expected to use advanced sensor technology. However, these new ADS would potentially encounter crashes with existing vehicles and road-side hardware due to sensor malfunction, for example. Little research exists that explores crash scenarios with the existing road-side hardware that go beyond impact conditions evaluated today.

The GMU-Team has previously developed generic Finite Element (FE) models of different size ADS using traditional steel materials, funded by the Department of Transportation (DOT) ⁴. The models are used to understand the performance of these new type of vehicles in run-off road crashes, i.e., when impacting road-side hardware devices. Subsequently, these models were used to study compatibility aspects when an ADS collides with a traditional vehicle. ⁵

NHTSA recently published a Notice of Proposed Rulemaking (NPRM) “Occupant Protection for Automated Driving Systems” that addresses potential rulemaking changes to vehicles with and without ADS functionality, such as the definition of driver and protections required when there is not a steering wheel or steering column in a motor vehicle.

OBJECTIVE

Use generic ADS vehicle models that can also be used for occupant transportation to study the effect of using plastics and composite materials instead of steel for select components. Crash configurations included run-off road conditions and frontal impact compatibility crash test scenarios.

Apply commonly used metrics, such as OLC, to estimate differences in occupant loads. Conduct integrated occupant vehicle simulation using a generic sled model and adequate interior component FE models.

¹ Park C-K, Kan C-D, Hollowell W T, and S.I. Hill, “Investigation of opportunities for lightweight vehicles using advanced plastics and composites,” Report No. DOT HS 811 692, NHTSA, Washington, DC, 2012
<http://www.nhtsa.gov/DOT/NHTSA/NVS/Crashworthiness/Plastics/811692.pdf>

² Park C-K, Achstetter T, Kan C-D, Hollowell W T, “Understanding of Numerical Polymer/Composite Material Models and Their CAE applications,” George Mason University Final Report, 2017

³ Hollowell W T, Kan C-D, Park C-K, Reichert R, Evaluation of the Safety Performance and Weight Reduction Using CFRP Modified Automotive Structures in NHTSA's Frontal Oblique Impact Test, ESV Conference, Eindhoven, Netherlands, 2019

⁴ Reichert R, Marzougui D, Kan C-D, “Simulations Between Non-Occupied Automated Driving Systems and Road-side Hardware”, Report Number : DOT HS 812 871, NHTSA, Washington, DC, 2020 URL :
<https://rosap.ntl.bts.gov/view/dot/54288>

⁵ Reichert R, Kan C-D, Park C-K, Crash Compatibility for Unoccupied Automated Driving Systems, NHTSA, 2022

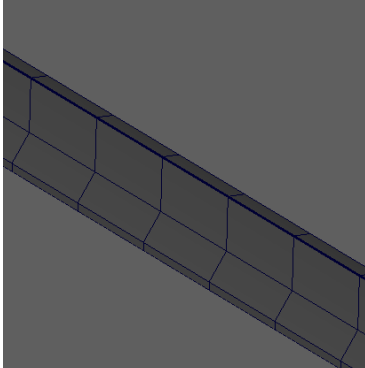

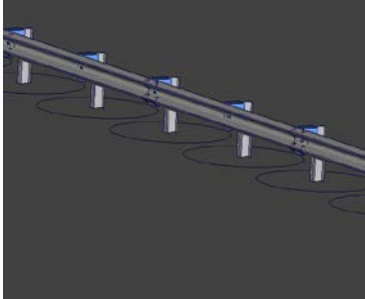

In addition, an advanced composite material model for shell elements is being developed and validated in cooperation with the Ohio State University (OSU) and Honda. The “MAT_213” material model will be made publicly available in LS-DYNA, once completed.

METHODS

Road-side Hardware

Current road-side testing practices are described in the Manual for Assessing Safety Hardware (MASH).⁶ Two representative road-side devices, i.e., (1) a rigid “New Jersey Barrier and (2) a W-beam guardrail, are shown in Table 1. Run-off-road crashes, which usually involve only a single vehicle, contribute to a large portion of fatalities and serious injuries to motor vehicle occupants.⁷ The NJB was selected to study the effect of different material concepts for ADS vehicles. Additional studies with the W-Beam guardrail and other road-side devices were conducted in previous research efforts.⁴

*Table 1.
Representative Road-side Hardware*

	Road-side Device	FE Model	Picture of similar Physical Device	Relevant References
1	New Jersey Barrier			Related studies and validation ⁸
2	W-Beam Guardrail			Related studies and validation ⁹

⁶ Manual for Assessing Safety Hardware (MASH) Transition, DOT Federal Highway Administration, Federal Register Volume 80, Issue 219, 80 FR 70288, Docket No. FHWA-2015-0008

⁷ Cejun Liu, Ph.D., and Tony Jianqiang Ye, “Run-Off-Road Crashes: An On-Scene Perspective,” Report No. DOT HS 811 500, NHTSA, Washington, DC, 2011

⁸ Marzougui et al, Crash Test & Simulation Comparisons of a Pickup Truck & a Small Car Oblique Impact into a Concrete Barrier, GMU, Fairfax (2014).

⁹ Marzougui et al, Evaluation of Rail Height Effects of the Safety Performance of W-Beam Barriers, NCAC, Ashburn (2007).

Traditional and ADS Vehicles

Vehicles recommended for testing under MASH are the 1100C small car, 1500A mid-size sedan, and the 2270P pick-up truck. FE models of a Toyota Yaris small car and a Chevrolet Silverado have been developed, validated, and used in previous research.⁴ Pictures of two conventional vehicles are shown in Figure 1. They were used as references in related research.⁴

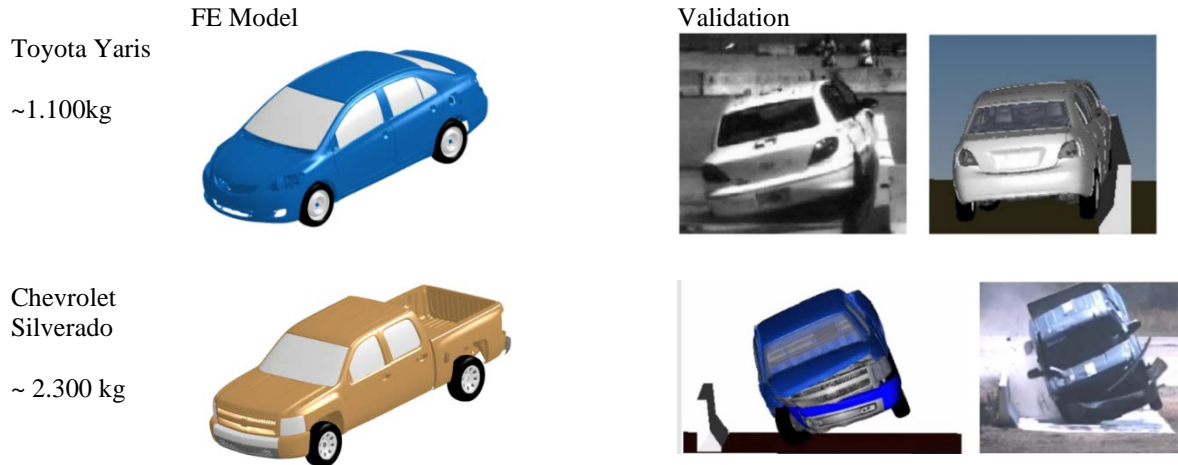


Figure 1. Conventional Vehicles

Other validated FE models that can be used as traditional vehicle references for material concept and other research studies include the 2014 Honda Accord¹⁰, 2015 Toyota Camry¹¹, and 2020 Nissan Rogue.¹² The 2015 Toyota Camry representing the sedan vehicle class and the 2020 Nissan Rogue representing the SUV vehicle class have been validated against existing pedestrian safety impact configurations, in addition to validation against frontal and side impact scenarios. ADS vehicles for this study are based on the two concepts shown in Figure 2. The mid-size ADS could be used to carry cargo or up to 5 occupants comparable to a sedan vehicle. The large ADS could be used to carry cargo or up to 10 occupants comparable to an airport shuttle, for example.



Figure 2. ADS Concepts

¹⁰ Singh H, “Vehicle Interior and Restraints Modeling”, EDAG Inc., Washington DC, 2017, https://www.nhtsa.gov/sites/nhtsa.gov/files/documents/812545_edagvehicleinteriorandrestraintsmodelingreport.pdf,

¹¹ Reichert R, Kan C-D, (2017). “Development of a 2015 Mid-Size Sedan Vehicle Model”. 11th European LS-DYNA Conference

¹² Reichert R, Mahadevaiah U, Fuchs L, Kan C-D, “Development of a 2020 SUV vehicle FE model”, 16th LS-DYNA Forum 2022, Bamberg, Germany, 2022. <https://www.ccsa.gmu.edu/models>

¹³ <https://www.theverge.com/mercedes-benz-vision-urbanetic-self-driving-electric-concept-design>, accessed June 2019

¹⁴ <https://venturebeat.com/swedens-einride-debuts-prototype-t-pod-an-autonomous-electric-truck-that-can-also-be-controlled-remotely>, accessed June 2019

Previously developed methods to develop generic ADS FE models included the transformation into an electric drive and the use of skateboard-type chassis. See Figure 3.

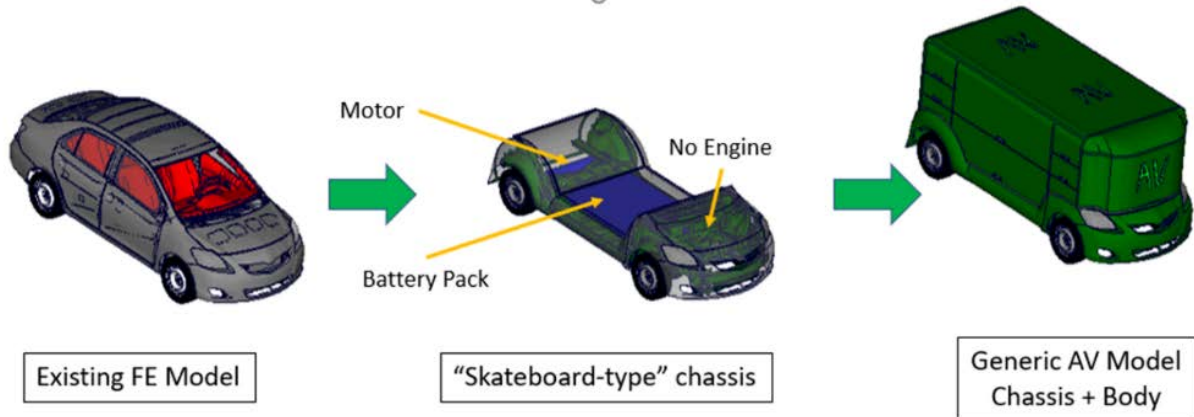


Figure 3. Development of Generic ADS Models

Existing ADS vehicle concepts served as a reference for the development of generic mid-size and large ADS vehicle models. For examples, see Figure 4.

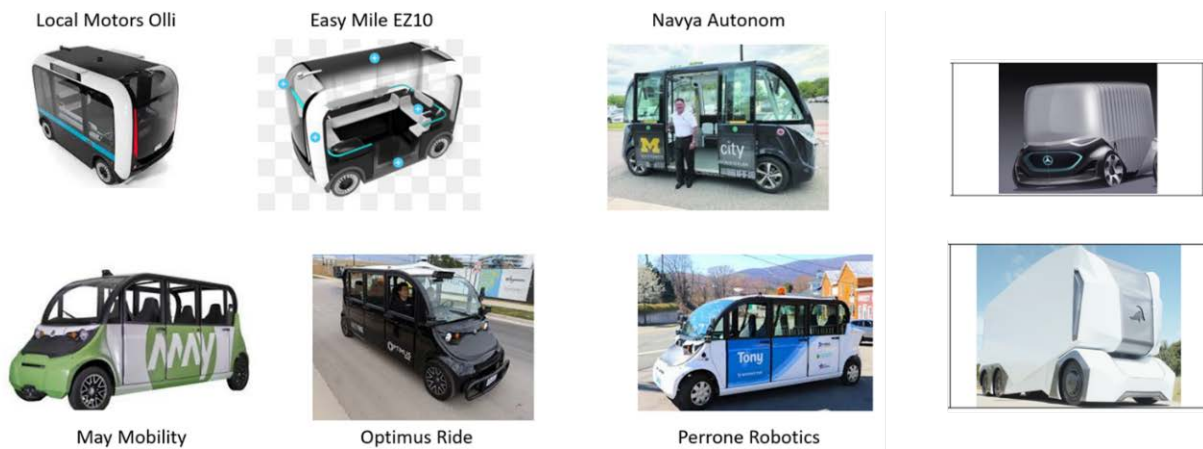


Figure 4. ADS Vehicle Concept Examples

Impact Configurations and Parameters

A standard impact into a NJB guardrail was conducted with vehicles of specified mass, at 100km/h impact speed and a 25° angle. Since impact scenarios with ADS vehicles are expected to differ in impact angle and impact speed, a wider range of parameters was studied. The three parameters are illustrated in Figure 5.

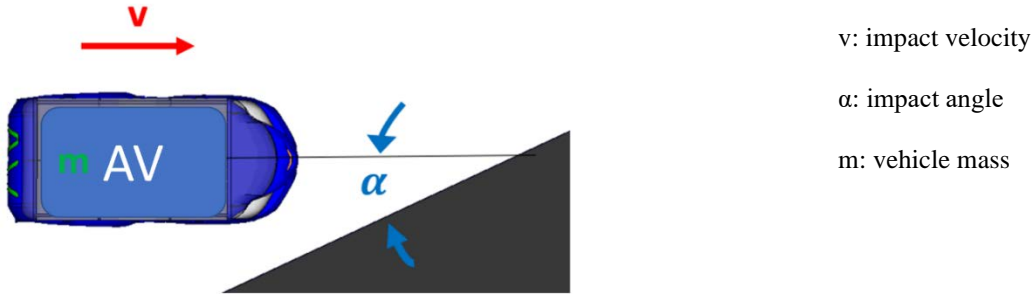


Figure 5. Impact Configuration and Parameters

Material Concepts

Steel, composite, and thermoplastic material concepts for the ADS vehicle body were considered, as shown in Figure 6.

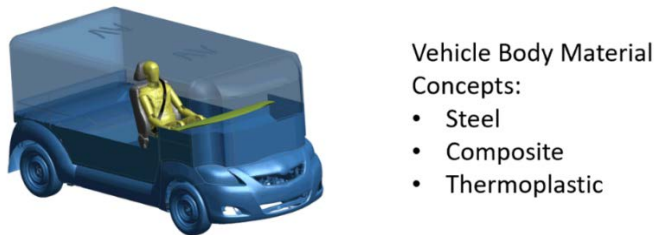


Figure 6. Generic Vehicle Model and Material Concepts

A braided carbon-fiber thermoset composite material has been used in previous projects.¹⁵ In addition, GMU has developed a material model of MAT 213 Shell Element version for implementation into LS-DYNA¹⁶. The development of the material model including failures has been completed and was integrated into the code.

Development of Component Models for Occupant Analysis

ADS vehicles are anticipated to allow unconventional seating configurations, such as rotated orientations. Therefore, the seat-belt D-ring will have to be integrated into the seat, rather than mounted at the vehicle structure’s B-Pillar, for example. Consequently, a FE model of a seat with integrated seatbelt has been developed, as shown in Figure 7, and used in previous research efforts.¹⁷

¹⁵ Park C-K, Kan C-D, Hollowell W T, and S.I. Hill, “Investigation of opportunities for lightweight vehicles using advanced plastics and composites,” Report No. DOT HS 811 692, NHTSA, Washington, DC, 2012
<http://www.nhtsa.gov/DOT/NHTSA/NVS/Crashworthiness/Plastics/811692.pdf>

¹⁶ Achstetter et al, “Development of a Composite Material Shell-Element Model for Impact Applications”, LS-DYNA Conference, 2020

¹⁷ Reichert, R. and Kan, C.-D., “Effect of Reclined and Rotated Seating for Automated Driving Systems,” SAE Technical Paper 2022-01-5048, 2022, doi:10.4271/2022-01-5048

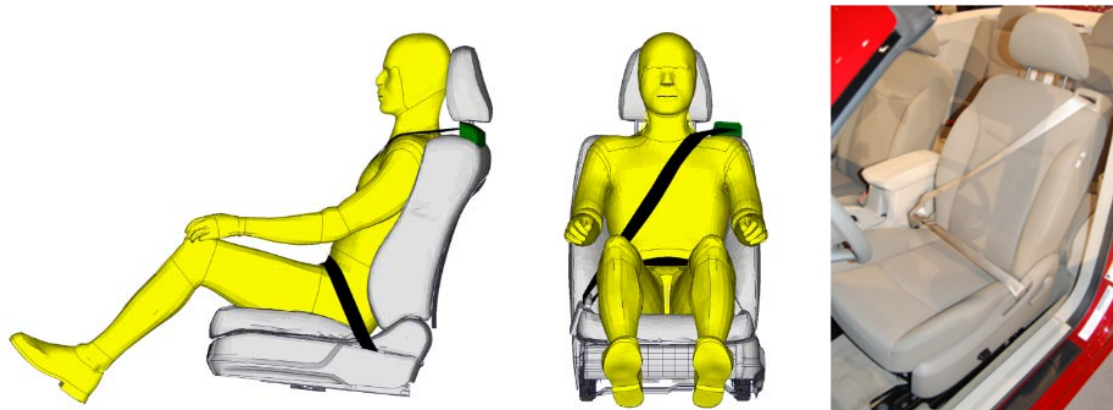


Figure 7. Seat with Integrated Seatbelt

“Seat-squash” and “seat-belt fitting” procedures are used to position respective occupants in the seat and to realistically place the seatbelt on the occupant.

Development of Component Models for Occupant Analysis

In preparation for subsequent studies using the developed generic ADS vehicle models with different material concepts in combination with interior and occupants, generic seat models have been developed. See Figure 8. They allow the study of a variety of unconventional seating arrangements including front-, side-, and rear-facing orientations.

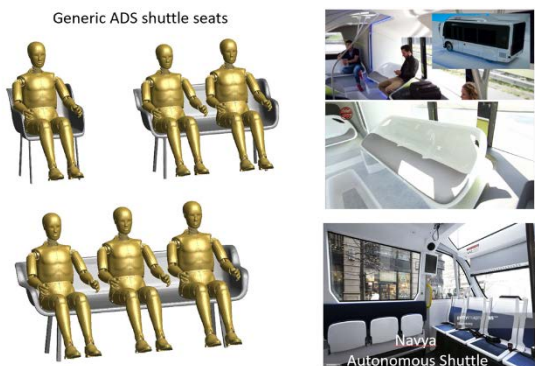


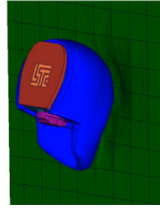
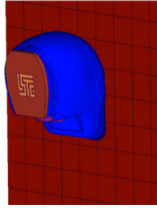
Figure 8. Generic Shuttle Seats

Development of FMVSS No. 201 Compliant Interior

Similarly, in preparation for subsequent studies using the developed generic ADS vehicle models with different material concepts in combination with interior and occupants, generic interiors were developed. FMVSS No. 201 requires vehicle interiors to be designed to produce a Head Injury Criterion, $HIC(d) < 1000$ when impacted by a Free Motion Head-form (FMH) at defined locations, angles, and impact speeds. Energy absorbing generic interior models with thermoplastic material characteristics were developed, that produced a $HIC(d)$ value below 800, as shown in Figure 9. Their effect in comparison to non-energy absorbing “rigid” interior concepts were studied in previous research.¹⁸

¹⁸ Reichert R, Kan C-D, Park C-K (2022, October). Crash safety considerations for speed-limited ADS shuttles (Report No. DOT HS 813 354). National Highway Traffic Safety Administration.

“Rigid” Surface
HIC(d) >> 1000



FMVSS 201
compliant surface
HIC(d) < 800

Figure 9. Development of FMVSS No. 201 Compliant Interior

Compatibility Assessment using EuronCAP’s MPDB

EuronCAP has introduced a frontal offset test procedure with a Mobile Progressive Deformable Barrier (MPDB)¹⁹ to assess the partner protection of a vehicle, as shown in Figure 10.

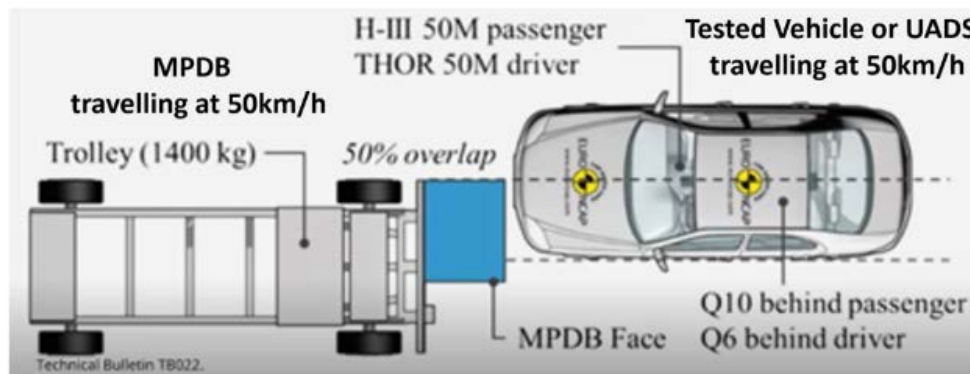


Figure 10. Vehicle Compatibility Rating Test Configuration

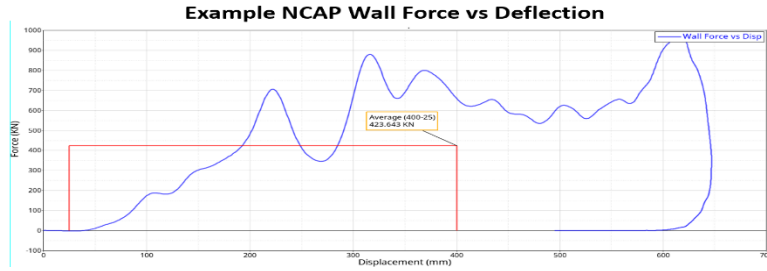
Respective MPDB FE models to assess the compatibility of traditional and ADS vehicles exist.²⁰ They were used to evaluate effect of different material concepts for ADS crash compatibility in frontal impact configurations.

Different compatibility metrics to assess partner protection exist. They include (1) bumper height assessment, which aims to enhance partner protection primarily through geometric matching of front structural components of cars and light trucks and vans; (2) Average Height of Force (AHoF), which is calculated from NCAP load cell measurements to quantify vertical geometric alignment of a vehicle; (3) Crush Work Stiffness (Kw400), a metric to quantify the front-end stiffness related to the crush energy absorbed by a vehicle in the first 400 mm of crush when impacting a rigid wall; (4) OLC criteria used by EuroNCAP, calculated from the velocity pulse of the MPDB.

The crush work stiffness (Kw400) was used in related research, to study baseline ADS vehicles and to develop variations with different compatibility characteristics. Details are outlined in the discussion section. The crush work stiffness is determined by calculating the area under the Force – Deflection (F-D) curve between 25 and 400 mm of front-end crush in a NCAP full frontal impact configuration, as shown in Figure 11.

¹⁹ Reichert R, Kan C-D, Park C-K, Crash Compatibility for Unoccupied Automated Driving Systems, NHTSA, 2022

²⁰ <https://lsdyna.ansys.com/lstc-barrier-models>. Accessed November 2022



$$\int_{25}^{400} F dx = \frac{1}{2} Kw400 [(400)^2 - (25)^2]$$

$$Kw400 = \frac{2F}{425}$$

Figure 11. Crush Work Stiffness Compatibility Metric; (a) Force-Displacement Example; (b) Kw400 Equation

The resulting stiffness value ‘K’ is termed Kw400, based on the equation outlined in Figure 11 (b), where F is the average of the total force on the barrier between 25 and 400 mm of vehicle crush. The first 25 mm of crush is ignored to account for soft materials and noise in the measured data. The maximum crush is limited to 400 mm to isolate the high inertial forces on the load cell wall due to engine contact.

EuroNCAP’s OLC metric was selected as the main metric to evaluate the energy absorbing characteristics of ADS vehicles. The OLC metric is derived from the virtual dummy responses estimated from a governing equation involving an assumed restraint system and a given vehicle crash pulse. This metric is independent of the actual dummy response. It assumes a virtual and uniform restraint system and that a virtual dummy will be in free-flight-phase along a displacement of 65 mm. In the restraining-phase an ideal restraint is assumed that would decelerate the occupant until the relative velocity between the occupant and the vehicle becomes zero. It is assumed that the distance between the vehicle and the occupant at point B is an additional 235 mm, as shown in Figure 12. For EuroNCAP’s compatibility assessment, the OLC is evaluated using a sliding scale between 25 g and 40 g. OLC values below 25 g result in four points and values above 40 g result in zero points.

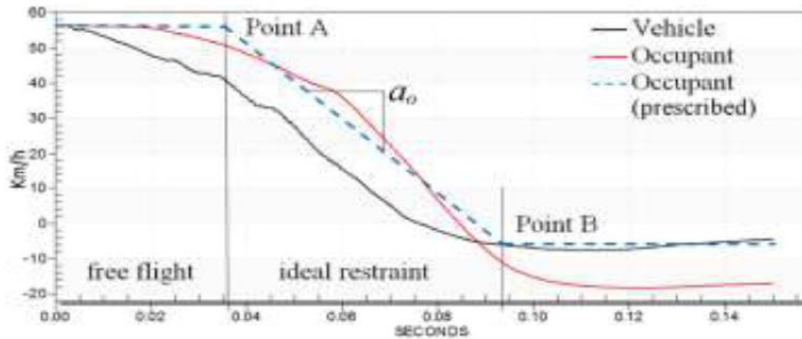


Figure 12. Occupant Load Criterion (OLC)

Bottoming out is defined as an area of the barrier that is 40 mm x 40 mm in height and width that has been penetrated by 630 mm or more. It is determined from a physical examination of the barrier face and vehicle.

RESULTS

Simulation Study 1 - Mid-size ADS impacting New Jersey Barrier (NJB)

Results using the mid-size ADS impacting the NJB are presented in this study. Figure 13 shows a top and side view of the developed mid-size ADS vehicle and impact configuration. Studied impact parameters and vehicle characteristics are listed below:

- Range of impact angles: 20°, 25°, and 30°
- Range of impact speeds: 25 mph, 35 mph, and 45 mph
- Material concepts for vehicle body (orange): steel, composite, and thermoplastic

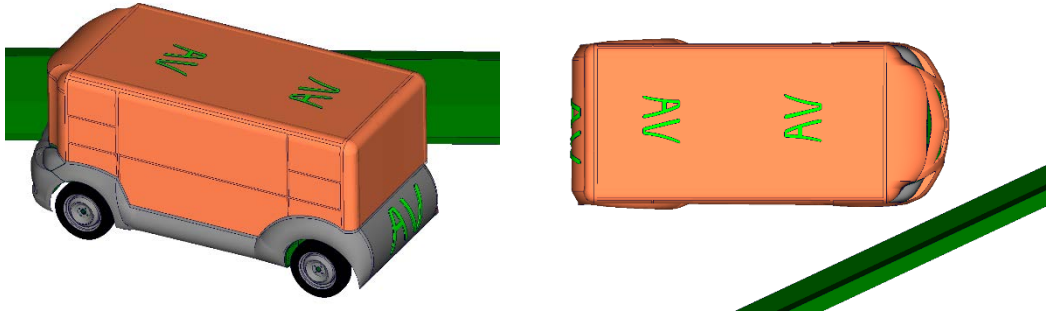


Figure 13. Mid-size ADS into NJB Impact Configuration

Simulations were conducted for all impact parameters and vehicle characteristics. For reference, an existing FE model representing a traditional sedan vehicle was evaluated, as shown in Figure 14. Vehicle mass and the height of the Center of Gravity (CG-z) are listed for the respective vehicles and material concepts.

Sedan (reference)	ADS (Thermoplastic)	ADS (Composite)	ADS (Steel)
Mass: 1200 kg	Mass: 973 kg	Mass: 996 kg	Mass: 1183 kg
CG (z): 549 mm	CG (z): 504 mm	CG (z): 526 mm	CG (z): 670 mm

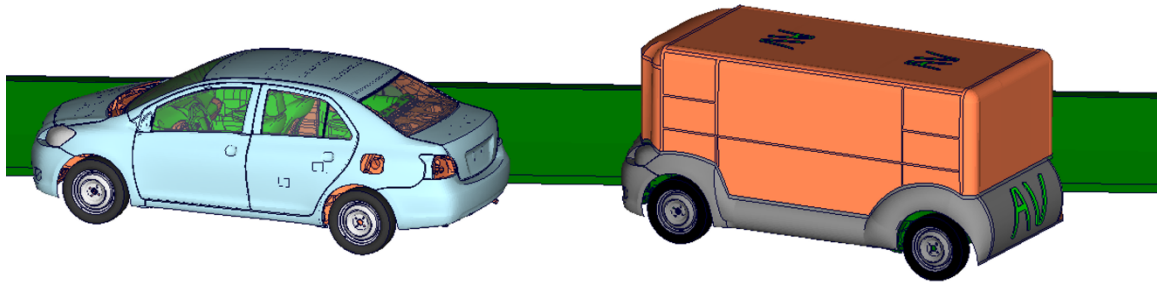


Figure 14. Comparison of traditional and mid-size ADS vehicle

Studies were conducted for impact velocities of 25 mph, 35 mph, and 45 mph of the mid-size ADSs into the NJB. For impacts at 25 mph, maximum roll angles well below the defined critical value of 40 degrees were observed for all cases. ADS with plastic or composite vehicle body tended to show marginally smaller roll angles compared to steel body for 25 mph impacts. See Figure 15.

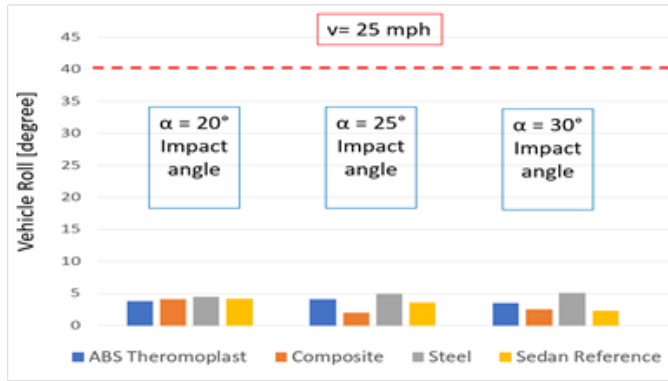


Figure 15. Mid-size ADS into NJB at 25 mph

For impacts at 35 mph, maximum roll angles below the defined criteria of 40 degrees were observed for all material concepts. ADS with a plastic or composite vehicle body showed clearly less critical roll angles compared to a steel body for all impact angles, especially for the 30° impact angle. See Figure 16.

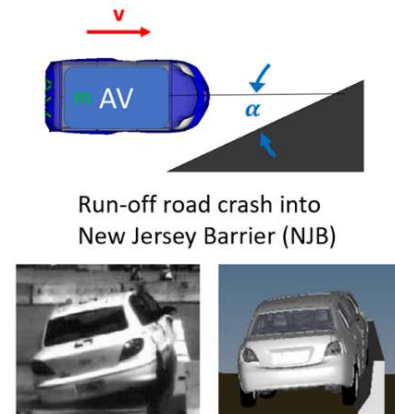
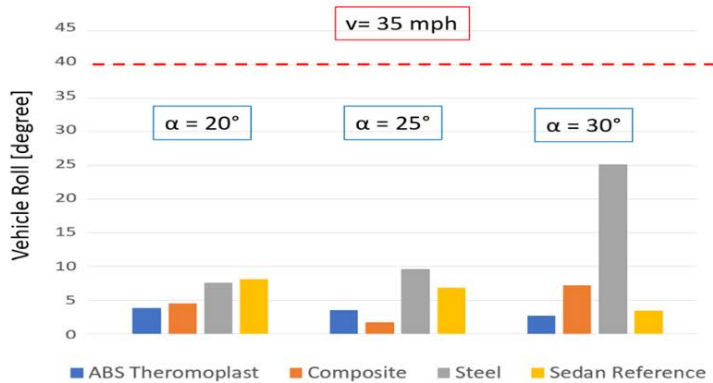


Figure 16. Simulation Study 1 – Mid-size ADS into NJB at 35 mph

For impacts at 45 mph, the ADS with a plastic or composite vehicle body again showed clearly less critical roll angles compared to a steel body for all impact angles, especially for the 30° impact angle. See Figure 17.

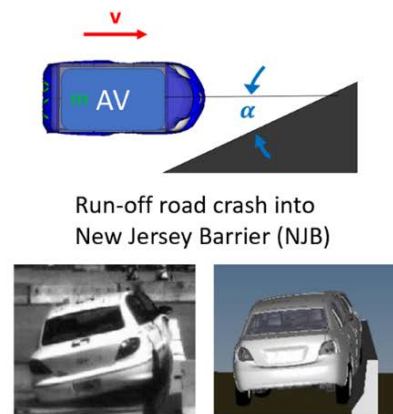
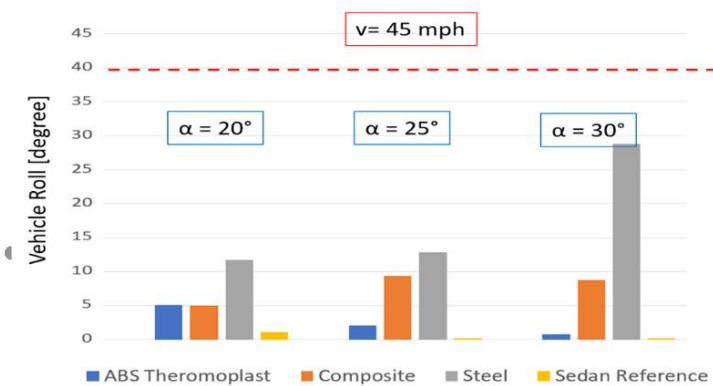


Figure 17. Simulation Study 1 – Mid-size ADS into NJB at 45 mph

Simulation Study 2 - Large-size ADS impacting New Jersey Barrier (NJB)

Figure 18 shows a front view of a Chevrolet Silverado reference vehicle impacting a NJB in simulation and full-scale test.

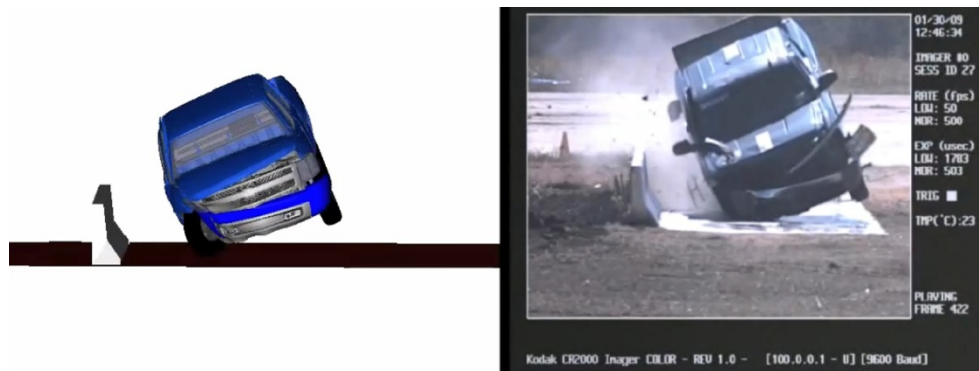


Figure 18. Large ADS Reference Vehicle impacting NJB (a) Simulation; (b) Test

Figure 19 illustrates studied impact parameters and vehicle characteristics used for the large ADS study.

- Range of impact angles: 20°, 25°, and 30°
- Impact speeds: 35 mph
- Material concepts for vehicle body: steel, composite, and thermoplastic

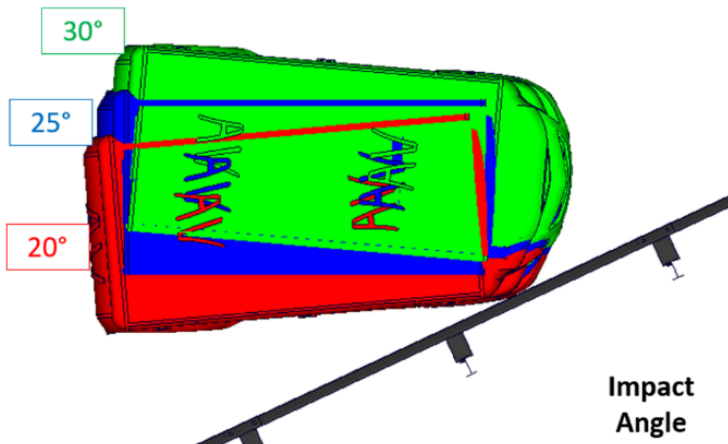


Figure 19. Large ADS with different impact angles

Table 2 summarizes the mass and height of the Center of Gravity (CG) for the SUV reference and the large ADS vehicles using different material concepts. Note that all ADS vehicles have a higher mass than the SUV reference vehicle due to their size with the steel version being the highest. Similarly, the CGs of the large ADS vehicles were higher than the CG of the Silverado reference SUV, with the steel version being the highest.

Table 2.
Large ADS: Mass and CG Comparison

	SUV (Reference)	Large ADS Thermoplastic	Large ADS Composite	Large ADS Steel
Mass [kg]	2,271	3,653	3,718	4,273
CG-z [mm]	732	764	789	975

The results for the simulation study 2 for impacts of the large ADS travelling at 35 mph into the New Jersey Barrier are shown in Figure 20. Maximum roll angles well below the defined criteria of 40 degrees were observed for all cases. ADS a with plastic or composite vehicle body showed significantly smaller roll angles compared to steel body.

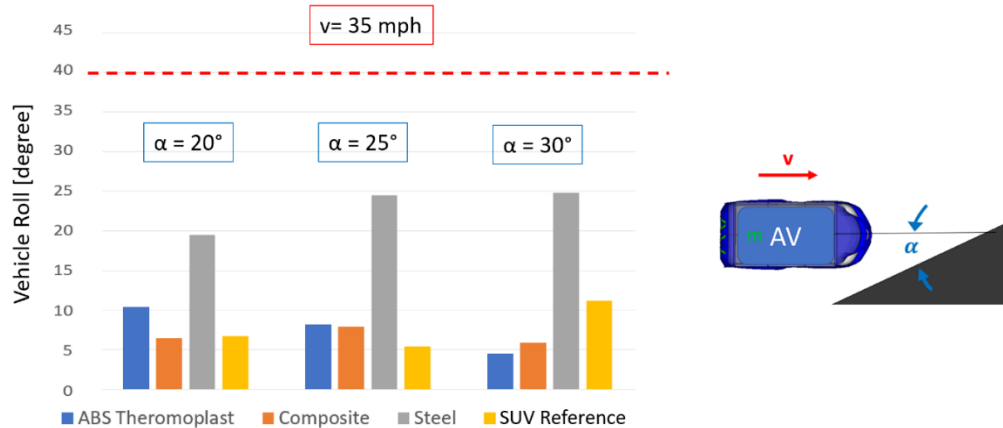


Figure 20. Simulation Study 2 – Large ADS into NJB

Simulation Study 3 – Mid-size ADS impacting NJB – Occupant Analysis

Vehicle pulses from the mid-size ADS vehicles with different material concepts impacting the NJB were recorded. The recorded vehicle pulses were then used to assess occupant injury risk with a previously developed generic sled model.¹⁶ The generic sled model includes relevant interiors and restraints and allows the analysis of occupant injury risk, as shown in Figure 21. An ADS vehicle allowing manual or automated driving mode was assumed. The study was conducted for an occupant seated on the driver seat with a steering wheel and driver airbag present.

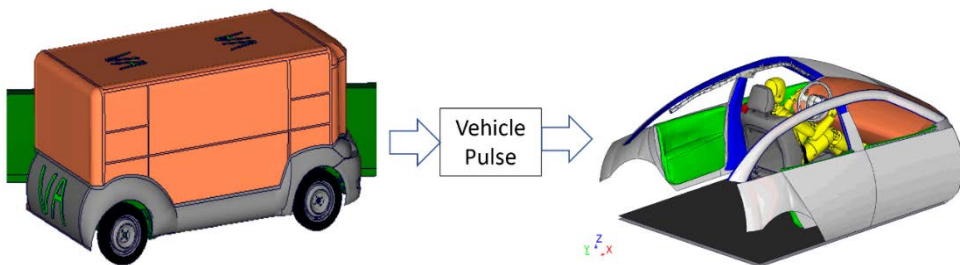


Figure 21. Evaluation Process of Occupant Responses using a Generic Sled Model

The generic sled model was developed to evaluate the effect of different vehicle pulses, seating orientations, and postures. It therefore assumes a seat-integrated restraints system. Dimensions, interior geometry, and package were adopted from a detailed finite element (FE) model of a 2014 Honda Accord²¹. The generic sled model exterior is represented by rigid parts, depicted in gray. Interior components with elastoplastic material and energy absorbing characteristics were used to allow for realistic occupant-to-vehicle interactions. This included a deformable floor, instrument panel, windshield, B-Pillar, and door trim components.

For the front-facing scenarios in the frontal impact scenario, interaction of the occupant with the seat, seatbelt, and airbag are dominant. In addition, interaction of the feet with the floor and the knees with the instrument panel affect occupant kinematics and loads.

²¹ H. Singh, "Vehicle Interior and Restraints Modeling", EDAG Inc., Washington DC, 2017

https://www.nhtsa.gov/sites/nhtsa.gov/files/documents/812545_edagvehicleinteriorandrestraintsmodelingreport.pdf, accessed July 7, 2021

The developed generic occupied sled model was used to evaluate the effect of different vehicle pulses recorded from impacts with the mid-size ADS with different material concepts. The 35mph impacts of the mid-size ADS and the reference Toyota Yaris structural vehicles into the NJB at a 25-degree angle were selected, as highlighted by the green frame in Figure 22.

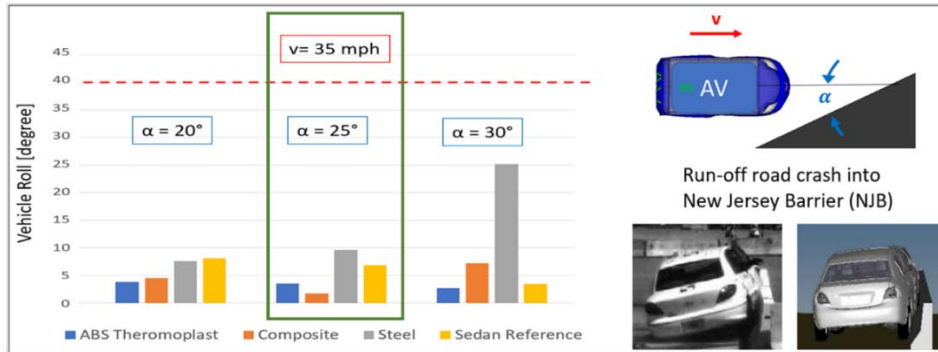


Figure 22. Simulation Study 2 – Mid-size ADS into NJB

In addition to the vehicle roll angle; vehicle pitch, vehicle yaw, and x-, y-, and z-pulses were recorded. The recorded motion was then applied to the previously developed generic sled model with a Hybrid 3 ATD on the driver seat, as shown in Figure 23.

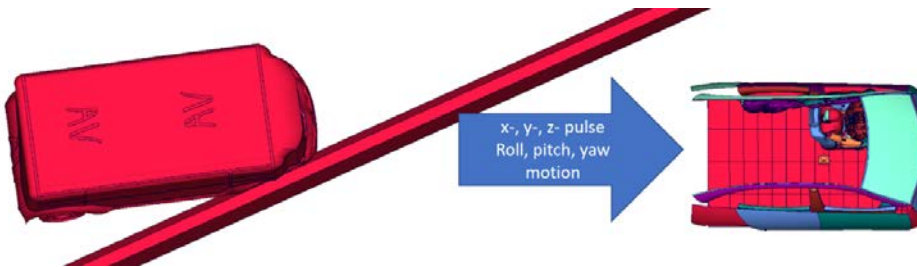


Figure 23. Mid-size occupant study: recorded motion from structural simulations applied to generic sled model

Figure 24 shows ATD and sled model kinematics 200ms after initial impact with the NJB for vehicle motion from ADS with steel body in gray and for vehicle motion from ADS with composite body shown in orange. Note that the lateral head trajectory tends to be marginally higher for the steel ADS motion compared to the composite ADS motion. Lateral head trajectory is relevant for far-side lateral impacts and is rated by EuroNCAP for side pole impact configurations, for example.

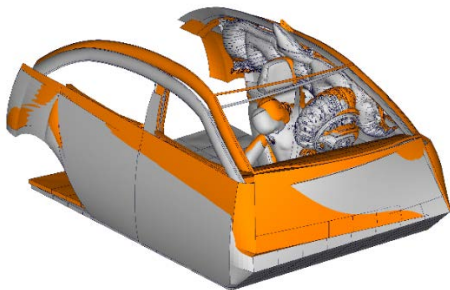


Figure 24. ATD and Sled Model Kinematics 200ms after Initial Impact with the NJB Example: Vehicle Motion from ADS with Steel Body (Gray) and Vehicle Motion from ADS with Composite Body (Orange)

Table 3 summarizes characteristic values of the Hybrid 3 ATD in the identical generic sled model interior environment with respective vehicle motions. Color coding is used to highlight the different material concepts studied. Reference values for the evaluated injury metrics, HIC, BRIC, chest deflection, and femur loads are shown

in the second column. Results for the mid-size ADS motion with an ABS, composite, and steel body are highlighted in blue, orange, and gray, respectively. Results when applying pulses from the Toyota Yaris sedan vehicle are highlighted in yellow.

Table 3.
Hybrid 3 ATD characteristic values

	Reference	ABS	Composite	Steel	Sedan
HIC	1000	68	68	70	69
BRIC	1.05	0.68	0.67	0.67	0.69
Chest [mm]	22	8	9	9	9
Femur left [N]	8558	822	691	656	804
Femur right [N]	8558	1231	1116	1267	1273

Note that all injury values are well below the documented reference values. Only small differences for the ATD metrics were observed when applying the vehicle motions from the respective ADS and sedan reference vehicle impacts into the NJB.

Simulation Study 4 - Compatibility Assessment

Compatibility metrics for the mid-size ADS with different material concepts were evaluated. Figure 25 shows the results for the EuroNCAP MPDB compatibility configuration. The impact of the vehicle using thermoplastic material for select components and a mass 3,653 kg with the MPDB resulted in an OLC value of 18. The same vehicle with composite material for selected components and a mass of 3,718 kg showed an OLC value of 19, while an OLC value of 22 was recorded for the baseline vehicle using steel with a mass of 4,273 kg. Lower OLC values indicate better compatibility. Hence, the use of thermoplastic and composite material resulted in lower vehicle mass and better compatibility metrics.

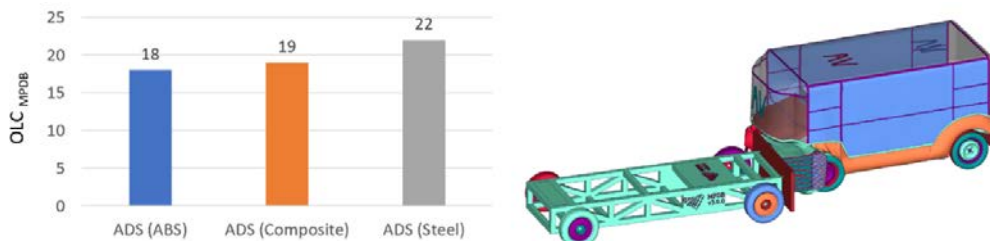


Figure 25. *OLC compatibility metric for midsize ADS with different material concepts*

ANCILLARY RESEARCH

In collaboration with Honda and OSU, material coupon specimen tests for a select composite material have been conducted. The validation and verification process using a previously developed LS-Dyna material model²² and the generated test data is ongoing. Specimen test series included tension, compression, and shear loading conditions. Tests were conducted quasi-statically, at different rates, different hysteresis load patterns, and different temperatures. The material model will be made publicly available, once completed. Additional information regarding the material model development process is documented in Appendix 1.

In addition to adequate material, state-of-the-art vehicle, occupant, and restraint modelling, realistic representation of battery modules will be essential to ensure crashworthiness of electric vehicles. Hence, a lithium-ion battery pack capable of capturing electrochemical, electromagnetic, and thermal-mechanical effects is currently being developed. Additional detail can be found in Appendix 2. The planned application of using the developed battery pack in context of the conducted research is discussed in the next section.

²² Tobias Achstetter, "Development of a Composite Material Shell-Element Model for Impact Applications," 2019, Dissertation, George Mason University

DISCUSSION

Effect of different material concepts

The use of different material concepts resulted in different total vehicle mass and CG location, which affected the vehicles' compatibility characteristics. For example, the large ADS vehicle using thermoplastic material for select components had a mass of 3,653 kg and a OLC of 18. The same vehicle with composite material concept had a mass of 3,718 kg and a OLC of 19, while the baseline vehicle using steel had a mass of 4,273 kg and an OLC of 22. Lower vehicle mass correlated with better partner-protection based on OLC metrics. Differences in OLC correlated with the difference in vehicle mass, which is considered small and can potentially be compensated by optimizing frontal vehicle structures. This is demonstrated by comparing differences in OLC and KW400 metrics for UADS vehicles with different structural characteristics from previous research²³, as shown in Figure 26.

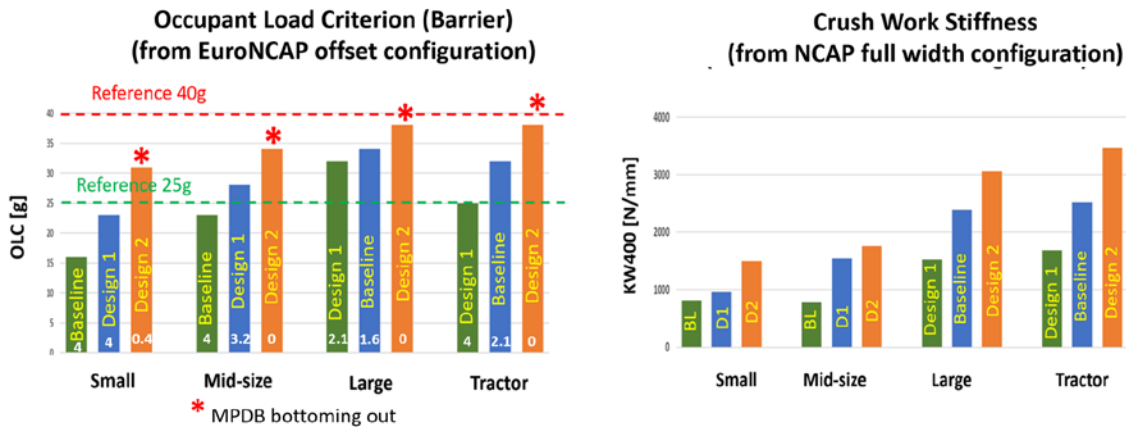


Figure 26. Summary of compatibility metrics for 4 UADS categories (a) OLC; (b) KW400

Two variations documented in the aforementioned previous research in addition to the baseline model for each of four UADS categories were developed by modifying the material strength and material thickness of relevant frontal structural components. Figure 26 (a) summarizes the compatibility characteristics for small, mid-size, large, and tractor UADS categories, based on the OLC, calculated from the MPDB barrier pulse in EuroNCAP's offset impact configuration. Reference lines representing an OLC of 25 g and 40 g are shown in green and red, respectively. In addition to the OLC, barrier bottoming out was evaluated. If bottoming out occurs, a 2-point penalty modifier applies. For example, if a vehicle generates an OLC of 32.5 g and barrier face bottoming out is observed, zero points would be given for the overall rating. The red asterisk on top of the design variations of the four UADS categories with the highest OLC values indicates that bottoming out was observed. The respective EuroNCAP score based on the OLC value and the bottoming out penalties is documented by the numbers, shown in white at the bottom of each bar. Figure 26 (b) summarizes the crush work stiffness (KW400) values for the respective baseline models and UADS variations, as calculated from the force versus deformation characteristics in the NCAP full overlap impact. Similar trends can be observed for the OLC and KW400 metrics.

Effect of Material Concepts on Risk of Roll-Over in NJB Impact

Lower vehicle mass and lower CG correlated with reduced risk of rollover, based on run-off road impact scenarios. Differenced in risk of rollover during a 30° NJB impact was observed for the large and mid-size ADS vehicles. Using thermoplastic or composite materials for select vehicle components of the large ADS resulted in maximum roll angles of 2° and 7°, respectively, versus 25° for the baseline steel version. Similarly, the reduction of maximum roll angle for the mid-size ADS is considered significant. Maximum recorded roll angle during a 45mph NJB impact was reduced from 28° to 1° and 9°, respectively, when using thermoplastic or composite materials compared to the

²³ Reichert R, Kan C-D, Park C-K, Crash Compatibility for Unoccupied Automated Driving Systems, NHTSA, 2022

baseline version using steel materials. In addition to using lightweight materials, optimizing suspension characteristics and CG location are considered important parameters influencing risk of rollover during run-off road crashes.

Use of Interior Sled Models in Combination with Recorded Vehicle Pulses

The documented methodology of using a generic sled model with interiors and restraints in combination with previously recorded vehicle pulses allowed for the study of the effect of different vehicle material concepts on occupant injury risk. Occupant metrics were mainly affected by the interior concept, which was identical for all three vehicles during the studied run-off road impact. Differences in occupant load was therefore small for all body regions and well below select reference criteria. HIC and BRIC head injury metrics were found to be similar when using different material concepts. Similarly, chest and lower extremity femur loads were considered to be of similar magnitude when using different material concepts. During the conducted simulation study, different maximum roll angles were observed, while no roll over occurred for any of the considered vehicles. Relevant differences in occupant injury risk can be expected if a roll over does occur.

The methodology of recording vehicle kinematics and applying relevant pulses to a generic interior sled model was found to be advantageous not only with respect to numerical efficiency. The technique allowed to understand the effect of different full vehicle structural kinematics while keeping all other occupant, interior, and restraint characteristics identical. Similar techniques were used for related research²⁴, where different seating concepts, seating arrangements, and interior concepts were studied for a variety of speed limited ADS shuttles for frontal, side, and rear impact crash scenarios. Examples are depicted in Figure 28.

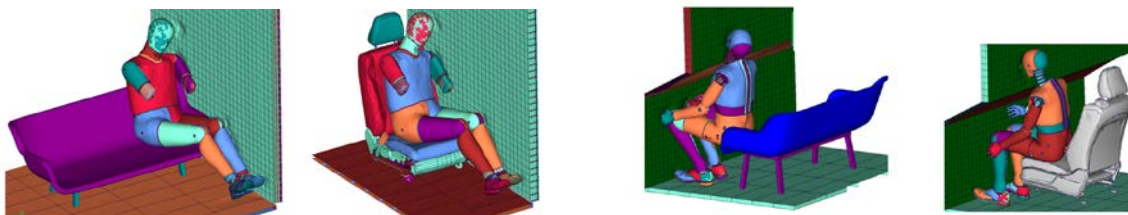


Figure 28. Examples of Generic Sled Application using Different Seating and Interior Concepts for (a) Side; (b) Frontal Impact Scenarios

Integrated Approach to Study Vehicle Material Concepts, Occupant Risk, and EV Safety

Ongoing research includes the combination of vehicle, material, occupant, and detailed battery pack FE models in an integrated approach. A FE model based on a Waymo self-driving vehicle is currently being equipped with relevant interiors, restraints, and battery pack components. The developed model allowed for the evaluation the effect of using different material concepts on structural deformation characteristics, occupant injury risk, and thermal run-away due to mechanical loads during a side pole impact, for example, as shown in Figure 29. Initial studies with a conventional vehicle were conducted to demonstrate the mass effect on vehicle intrusion, as shown in Figure 29 (d). Increased vehicle mass resulted in increased intrusion. Similar effects are expected when studying different material concepts in combination with a ADS vehicle. Consequently, the increased risk of battery pack damage can be anticipated, for increased structural intrusion, depending on the material concept used, for example.

²⁴ Reichert R, Kan C-D, Park C-K (2022, October). Crash safety considerations for speed-limited ADS shuttles (Report No. DOT HS 813 354). National Highway Traffic Safety Administration.

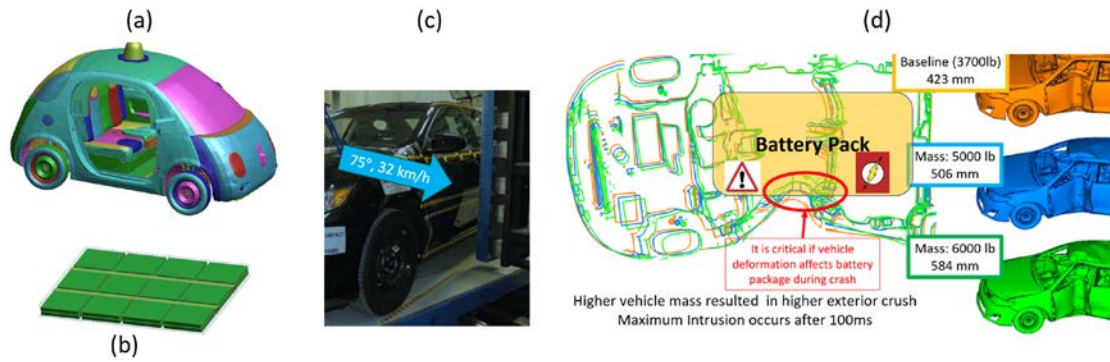


Figure 29. Waymo Self-driving Vehicle; (b) Multi-physics Battery Pack; (c) Side pole Impact; (d) Initial Study to Determine Mass Effect on Intrusion

Limitations

The same vehicle design and underlying structures were used during the study where standard steel materials were replaced with thermoplastic and composite materials, i.e. no optimization towards the respective material concept was performed.

CONCLUSION

The conducted research and the methods used demonstrate how simulation tools can contribute to assessing new type of ADS vehicle designs. Material concepts that resulted in a smaller vehicle mass tended to show better partner protection. Reduced vehicle mass and the corresponding lowered CG tended to reduce the risk of roll over. The interior concept, which was the same for three ADS vehicle variations studied, was the main factor for producing similar occupant injury metrics for the evaluated impact scenario.

ACKNOWLEDGEMENT

The authors wish to acknowledge the American Chemistry Council (ACC) for providing the main funding for this research. We also wish to acknowledge ACC's Gina Oliver and Barb Robertson for their technical and administrative support for this project. We also wish to acknowledge the National Highway Traffic Safety Administration (NHTSA) for the funding of their related research mentioned in this paper. Finally, we wish to acknowledge Honda which provided the main funding for the finite element material model development.

APPENDIX 1

COMPOSITE MATERIAL MODEL DEVELOPMENT

Introduction

Since the predictability of the existing analytical composite material models was not satisfactory in the application of high-velocity impact simulations, a team of George Mason University, Arizona State University, Ohio State University, the National Aeronautics and Space Administration, and the Federal Aviation Administration have collaborated to develop a new composite material model in LS-DYNA for high-velocity impact simulations.

As a result, *MAT_213 in LS-DYNA has been developed. *MAT_213 is an orthotropic constitutive model developed with strain hardening, non-associated plasticity, Tsai-Wu yield surface, and the second Tsai-Wu surface as flow surface. It uses tabulated hardening curves based on experimental material test data. It has three failure modes, such as Tsai-Wu Failure Criterion, Puck Failure Criterion, and Generalized Tabulated Failure Criterion. A damage model accounts for decreasing strength/stiffness. It could simulate pure linear material behavior with tension-compression asymmetry. In addition, the model includes a stochastic analysis function. Initially, it was developed for solid elements. Currently, *MAT_213 (V1.3.5) is available in a developing version to AWG (Aerospace Working Group) and sponsors (Honda). Soon, it will be available in future version of LS-DYNA R13 to the public.

After developing and implementing *MAT_213 into LS-Dyna, a dataset for T800/F3900 composite was developed. A tabulated experimental input dataset was created by conducting a series of material tests and simulations to satisfy the input requirements for the three sub-models' deformation, damage, and failure. For the deformation model, twelve (12) material coupon tests at various strain-rate and temperature combinations are needed, as shown in Figure 30. For the damage and failure models, additional test series are needed.

Test Description	Resulting Input for MAT_213
1-direction Tension	σ_{11}^T vs ϵ_{11}^T , $(\epsilon_{11})_y^T$, $(\sigma_{11})_y^T$, (ν_{12}, ν_{13}) , (ν_{12}^p, ν_{11}^p)
2-direction Tension	σ_{22}^T vs ϵ_{22}^T , $(\epsilon_{22})_y^T$, $(\sigma_{22})_y^T$, (ν_{23}, ν_{21}) , (ν_{23}^p, ν_{21}^p)
3-direction Tension	σ_{33}^T vs ϵ_{33}^T , $(\epsilon_{33})_y^T$, $(\sigma_{33})_y^T$, (ν_{32}, ν_{31}) , (ν_{32}^p, ν_{31}^p)
1-direction Compression	σ_{11}^C vs ϵ_{11}^C , $(\epsilon_{11})_y^C$, $(\sigma_{11})_y^C$, (ν_{12}, ν_{13}) , (ν_{12}^p, ν_{13}^p)
2-direction Compression	σ_{22}^C vs ϵ_{22}^C , $(\epsilon_{22})_y^C$, $(\sigma_{22})_y^C$, (ν_{23}, ν_{21}) , (ν_{23}^p, ν_{21}^p)
3-direction Compression	σ_{33}^C vs ϵ_{33}^C , $(\epsilon_{33})_y^C$, $(\sigma_{33})_y^C$, (ν_{32}, ν_{31}) , (ν_{32}^p, ν_{31}^p)
1-2 Plane Shear	σ_{12} vs ϵ_{12} , $(\epsilon_{12})_y$, $(\sigma_{12})_y$
2-3 Plane Shear	σ_{23} vs ϵ_{23} , $(\epsilon_{23})_y$, $(\sigma_{23})_y$
1-3 Plane Shear	σ_{13} vs ϵ_{13} , $(\epsilon_{13})_y$, $(\sigma_{13})_y$
1-2 Plane 45° Off-axis tension/compression	σ_{45}^{1-2} vs ϵ_{45}^{1-2} , $(\epsilon_{45}^{1-2})_y$, $(\sigma_{45}^{1-2})_y$
2-3 Plane 45° Off-axis tension/compression	σ_{45}^{2-3} vs ϵ_{45}^{2-3} , $(\epsilon_{45}^{2-3})_y$, $(\sigma_{45}^{2-3})_y$
1-3 Plane 45° Off-axis tension/compression	σ_{45}^{1-3} vs ϵ_{45}^{1-3} , $(\epsilon_{45}^{1-3})_y$, $(\sigma_{45}^{1-3})_y$

Figure 30. Material coupon test series for MAT_213

Figure 31 shows an example of a material coupon specimen.

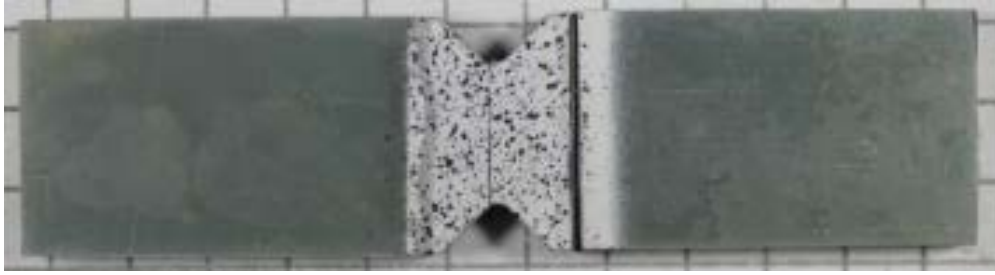


Figure 31. Material coupon specimen example

Honda R&D funded GMU to develop and validate the shell element version of *MAT_213 in LS- DYNA for automotive crash application in four phases. The first phase is to develop verify the code has been completed. Ongoing work during Phase 2 includes the characterization of a material law for a composite material based on coupon testing. During Phase 3 a comparison of different discretization techniques when used in conjunction with *MAT_213. Finally, validation of the material model based on component testing will be conducted during phase 4.

Composite material model validation

Ballistic impact conditions were selected for quality of material data and to validate robustness of the material model. Physical tests were conducted at NASA-GRC using a 50g projectile and unidirectional T800/F3900. Sixteen (16) fully integrated elements through the thickness and cohesive elements between all layers were modeled. The model consisted of ~400,000 shell elements and ~300,000 solid cohesive elements.

LS-DYNA material model *MAT_213 shell routine development work was previously conducted by (Achstetter, 2019)²⁵, which included:

- Develop and implement plane stress plasticity algorithm by stress projection
- Develop and implement orthotropic VE-VP algorithm with non-linear visco-elasticity.
- Develop and implement strain rate smoothing algorithm
- Update tabulated failure model
- Develop and implement stochastic option
- Improve robustness of plasticity algorithm (radial return ‘backup’ solution)

The developed material model was used to simulate three cases from a test series with different impact and rebound/exit velocities, as shown in Figure 32.

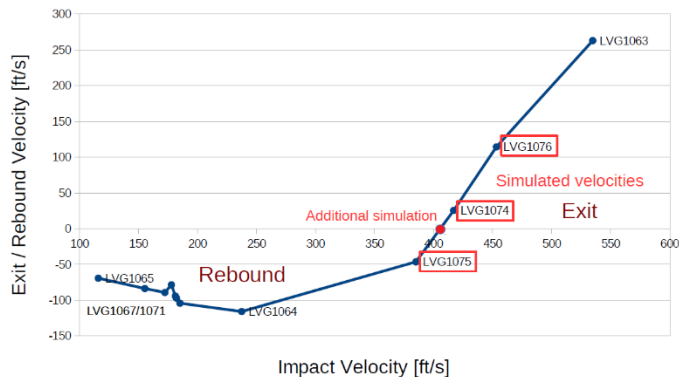


Figure 32. Exit / rebound velocity versus impact velocity test series and select simulations

Delamination characteristics were well captured as shown in Figure 33.

²⁵ Tobias Achstetter, “Development of a Composite Material Shell-Element Model for Impact Applications,” 2019, Dissertation, George Mason University

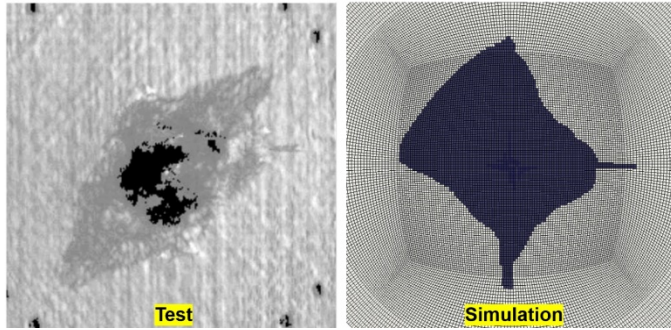


Figure 33. Comparison of delamination in test (LVG1075) and respective simulation

Overall good correlation when comparing the composite fracture and delamination between test and simulation was observed, as shown in Figure 34.

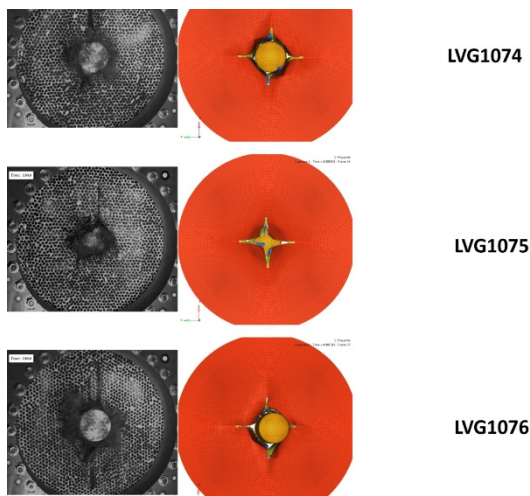


Figure 34. Comparison of test and simulation for different impact velocities

C-Channel Crush

Honda conducted C-Channel crush tests using composite layup [45/-45/0/90]. Two modeling approaches were applied. In approach 1, one element through the thickness and 8 integration points were defined using *MAT_58. In approach 2, one element per ply and 2 integration points were specified using *MAT_213. It was found that MAT_213 compares better with the test results showing closer failure behavior and more localized stress concentration at the crush area, as shown in Figure 35.

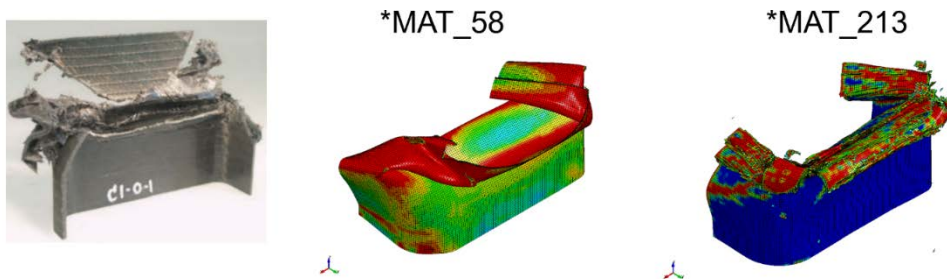


Figure 35. C-Channel Crush (a) Test; (b) Mat_58; (c) Mat_213

APPENDIX 2

BATTERY MODELLING

Lithium Battery Background

The Nobel Prize in Chemistry 2019 was awarded jointly to John B. Goodenough, M. Stanley Whittingham, and Akira Yoshino for the development of lithium-ion batteries. The history of lithium-ion battery can be dated back to 1970s. Whittingham created the first working, rechargeable metallic Lithium battery in 1976. In 1979/1980, John B. Goodenough discovered that Lithium cobalt oxide could serve as a cathode material in a “ion transfer cell” configuration. In 1985, Akira Yoshino identified that certain qualities of petroleum coke can be used as anode material and created the first commercialized lithium-ion battery, which is the Sony rechargeable battery. Since then, lithium-ion battery technology has rapidly progressed. For example, modern lithium-ion batteries are composed by multiple layers of thin membranes. A typical cell consists of a layer of aluminum coated with Lithium manganese oxide, a polyethylene separator, and a layer of copper coated with graphite. All these membranes are very thin, and they are rolled up as to form either a cylinder shape or a porch shape. Additional protective circuit is often necessary for safe operation.

Lithium-ion battery’s advantages are high energy density, high open-circuit voltage, low internal resistance, long cycle life, and quick charging. The disadvantage is the safety issues. Fire or explosion may occur when overcharge occurs, when exposed to high temperature, or when short circuit or puncture occurs. Examples include fire in some Tesla electric cars, initiated from the battery after impact. Lithium-ion battery fires are also reported on cellphones, drones, and electric bicycles and scooters.

The development of reliable and robust battery models for simulating their behavior in crashes involving electric vehicles (EV) is needed. To address safety related issues, GMU has started to develop a lithium-ion battery FE model that can predict battery failure in EV Crash impacts and other high velocity impact applications. The battery model method adopted is aimed to allow computationally efficient simulations for engineering applications.

Lithium Battery Modeling Approach

To capture the physics of a lithium-ion battery cell in a fully coupled analysis, three aspects must be addressed:

- Electrochemical
- Electromagnetic
- Thermal-mechanical

Different battery cell verification tests allow validation of a battery cell FE model. They may include the three-point bending test to validate mechanical behavior, a battery circuit test to verify electrical performance, and a punch test at high and low temperatures to validate combined mechanical and thermal behavior. Figure 36 shows promising initial results of a hemispherical punch test and a simulation. The force versus displacement comparison depicts reasonably good correlation using material properties and test results from literature.

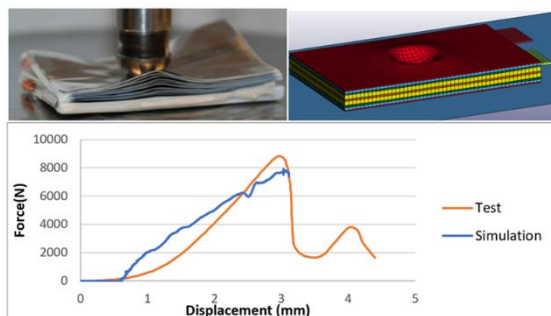


Figure 36. Physical punch test (upper left); simulation result (upper right); and test versus simulation force-displacement comparison (bottom)

To verify combined thermal and electrical predictability capabilities of a FE model, the external short circuit test can be used. Figure 37 shows an example of the electrical current density distribution for the preliminary FE model.

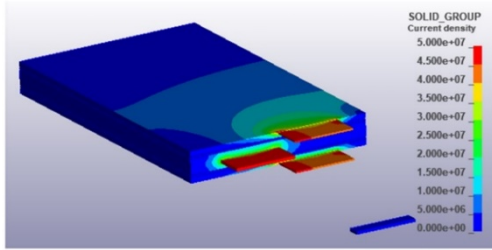


Figure 37. Electric current after external short circuit

Figure 38 shows the volumetric heat power during an external short circuit using the same FE model.

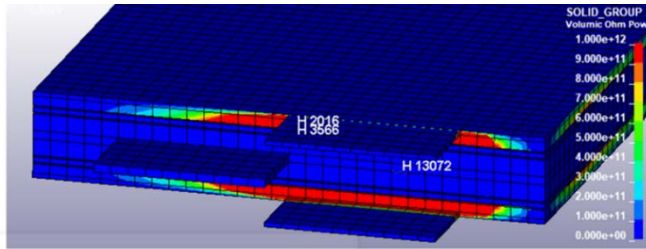


Figure 38. Volumetric heat power during an external short circuit

Figure 39 shows a so-called coated cathode material test, where the material coupon is placed in a thermal chamber to generate data for a separator test with elevated temperatures. This setup is currently being evaluated.

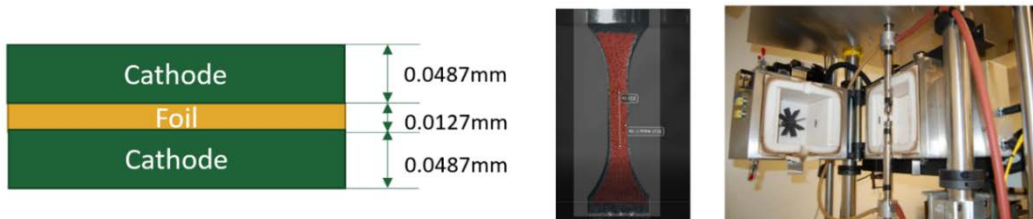


Figure 39. Volumetric heat power during an external short circuit

Lithium battery modeling from cell to module level

Modeling multi physics of an individual lithium battery cell is well understood and can be considered state-of-the-art. Significant progress of modeling two battery cells in series has been made, as shown in Figure 40. Promising results when comparing a two cell “battery pack” with respective test results were achieved. A so-called Randle’s circuit voltage source was used.

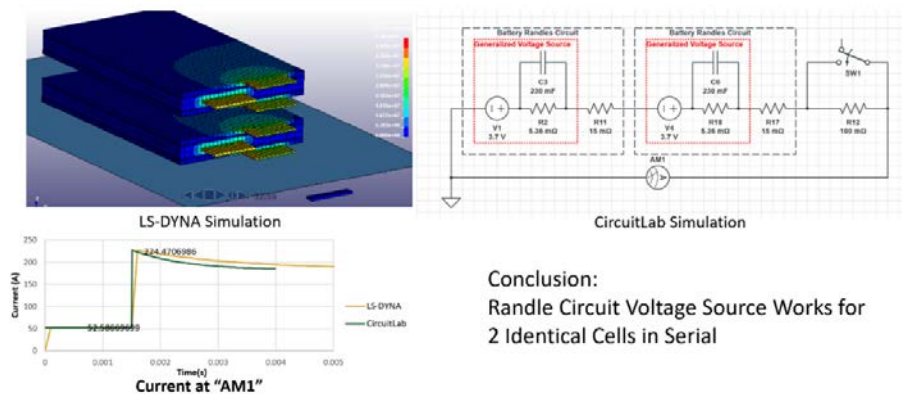


Figure 40. Randle’s circuit voltage source works for 2 DIFFERENT cells in serial

Similar to the two cells in serial evaluation, a two cell in parallel configuration was studied, as shown in Figure 41.

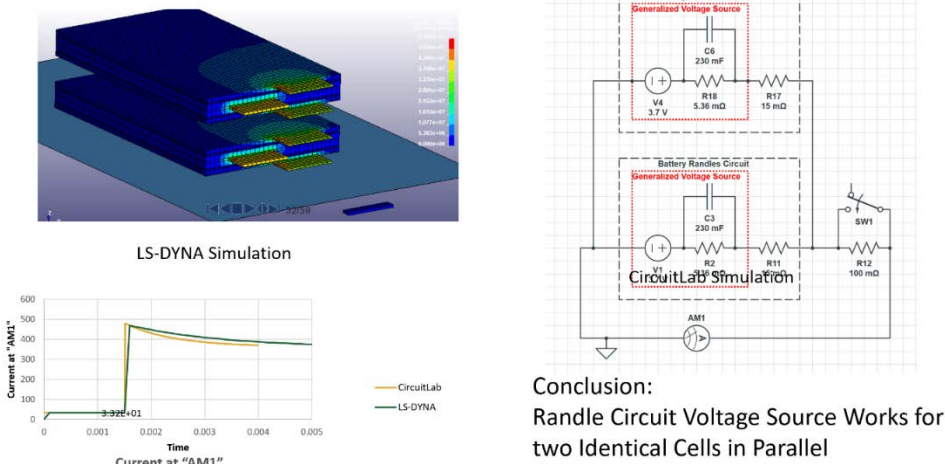


Figure 41. Randle’s circuit voltage source works for 2 DIFFERENT cells in parallel

Being able to combine two cells makes scalability and therefore modeling of a detailed battery pack with multiple individual cells realistic. The findings have been published in a journal paper by (Wang et. al., 2022).²⁶

Lithium Battery Modeling Outlook

The development and validation of a lithium battery pack is ongoing. The selected modelling technique will allow to evaluate electric vehicles during a crash event and provide a step-by-step approach to capture the thermal runaway condition, for example.

²⁶ Leyu Wang, Chenxi Ling, Cing-Dao Kan & Chi Yang. 2022. “A coupled thermal electrical mechanical analysis for lithium-ion battery.” Journal of Micromechanics and Molecular Physics. <https://www.worldscientific.com/doi/abs/10.1142/S2424913021420108?journalCode=jmmp>